This is a repository copy of *An approximate stochastic dynamics approach for nonlinear structural system performance-based multi-objective optimum design*.

White Rose Research Online URL for this paper:
http://eprints.whiterose.ac.uk/154385/

Version: Accepted Version

Article:

An approximate stochastic dynamics approach for nonlinear structural system performance-based multi-objective optimum design

Ioannis P. Mitseas[1*], Ioannis A. Kougioumtzoglou[2], M. Beer[3,1+,4]

[1]Institute for Risk and Uncertainty,

University of Liverpool,

Brodie Tower, Brownlow Street, L69 3GQ, Liverpool, United Kingdom.

e-mail: [*]iomitsea@liv.ac.uk,[+]mbeer@liv.ac.uk

[2]Department of Civil Engineering and Engineering Mechanics,

The Fu Foundation School of Engineering and Applied Sciences,

Columbia University,

500 West 120th Street, New York, NY 10027, USA.

e-mail: ikougioum@columbia.edu

[3]Faculty of Civil Engineering and Geodetic Science,

Leibniz University Hannover,

Callinstrabe 34, 30167, Hannover, Germany

e-mail: beer@bauinf.uni-hannover.de

[4]Department of Geotechnical Engineering,

Tongji University,

Shanghai 200092, China

Abstract.

A novel approach for structural system optimal design considering life cycle cost is developed.

Specifically, a performance-based multi-objective design optimization framework for nonlinear/hysteretic multi-degree-of-freedom (MDOF) structural systems subject to evolutionary stochastic excitation is formulated. In the core of the stochastic structural analysis component of the proposed framework lies an efficient approximate dimension reduction technique based on the concepts of statistical linearization and of stochastic averaging for determining the non-stationary system response amplitude probability density functions (PDFs); thus, computationally intensive Monte Carlo simulations are circumvented. Note that the approach can readily handle stochastic excitations of arbitrary non-separable evolutionary power spectral density (EPSD) forms that exhibit strong variability in both the intensity and the frequency content. Further, approximate closed-form expressions are derived for the non-stationary inter-story drift ratio amplitude PDFs corresponding to each and every DOF. In this regard, considering appropriately defined damage measures structural system related fragility curves are determined at a low computational cost as well. Finally, the structural system design optimization problem is formulated as a multi-objective one to be solved by a genetic algorithm based approach. A building structure comprising the versatile Bouc-Wen (hysteretic) model serves as a numerical example for demonstrating the efficiency of the proposed methodology.

Keywords: Nonlinear stochastic dynamics, Evolutionary power spectral density, Hysteresis, Statistical linearization, Performance-based earthquake engineering, Stochastic averaging, Multi-objective optimization

1 INTRODUCTION

Most structures and civil infrastructure systems are subject to excitations that exhibit strong variability in both the intensity and the frequency content. Clearly, a realistic system analysis and design necessitates the representation of this class of loads by non-stationary stochastic processes

[1,2,3]. Further, structural systems under severe excitations, such as earthquakes, can behave in a nonlinear manner exhibiting a hysteretic restoring force-displacement characteristic. Thus, a sustained challenge in the area of structural dynamics has been the efficient analysis and design of nonlinear/hysteretic systems/structures under evolutionary stochastic excitation.

Performance-based earthquake engineering (PBEE) aims at providing information for facilitating risk-based decision-making via performance assessment and design methods that properly account for the presence of uncertainties [4,5]. In general, the PBEE framework includes four basic stochastic analysis components (see section 3) which address the issue of stochastic structural design in a comprehensive and consistent manner. Considering the last component of a PBEE analysis, that of stochastic loss analysis, the seismic life-cycle cost is usually employed as a decision variable [6]. Indicatively, in [7], Kong and Frangopol addressed the bridge maintenance schedule optimal design problem and estimated the life-cycle cost performance. Further, adopting a median global Park-Ang damage index, Ang and Lee [8] considered repair costs for various ground motion intensity levels for the case of reinforced concrete buildings. In [9-10], a probabilistic multi-objective optimization framework was applied for the life-cycle cost optimal seismic design of steel structures. Further, Taflanidis and Beck [11] focused on assessing the performance of passive dissipative devices by utilizing an efficient simulation approach within a performance-based seismic design framework that optimized the expected life cycle cost of structural systems. Next, Takashi et al. [12] relied on a Monte Carlo simulation approach for assessing the life-cycle cost of a structural system equipped with damping devices.

Focusing on the stochastic structural/damage analysis components of a PBEE framework, several approaches have been developed for relating the seismic hazard to the system fragility and for producing corresponding fragility curves, i.e. probabilities of exceeding specified damage

states given an intensity measure (IM) value. These range from the ones that employ a limited number of nonlinear time-history analyses with prescribed IM level compatible scaled real earthquake records [13], to the ones that employ standard or efficient Monte Carlo simulation (MCS) based methodologies such as importance/line sampling, and subset simulation [14,15,16]. Nevertheless, note that there are cases where the computational cost of the MCS based techniques can be significantly high; thus, rendering their use computationally cumbersome, or even prohibitive. Clearly, there is a need for developing approximate analytical and/or numerical techniques for determining efficiently the response and reliability statistics of nonlinear systems subject to stochastic excitation [1,2,17-19]. Nevertheless, although there is a considerable body in the literature referring to the development of such techniques there are limited results related to adopting and implementing such techniques for efficient fragility analysis applications. An interesting contribution in this regard is the work by Der Kiureghian and Fujimura [20] where an efficient tail-equivalent linearization based approach was applied for fragility analysis of a nonlinear building structure.

In this paper, a performance-based multi-objective design optimization framework for nonlinear/hysteretic MDOF structural systems subject to evolutionary stochastic earthquake excitations is formulated. In the core of the stochastic structural analysis component lies an efficient approximate analytical dimension reduction approach for determining the system response evolutionary power spectral density (EPSD) matrix based on the concepts of statistical linearization and stochastic averaging [18]; thus, computationally intensive Monte Carlo simulations are circumvented. Note that the approach can readily handle stochastic excitations of arbitrary EPSD forms, even of the non-separable kind. Further, approximate closed-form expressions are derived for the non-stationary response amplitude PDFs of the inter-story drift

ratios (IDRs) corresponding to each and every DOF. In this regard, considering appropriately defined damage measures structural system related fragility curves are determined at a low computational cost as well. Further, note that the multi-objective optimization [21] allows for objectives that exhibit potentially conflicting requirements to be treated simultaneously. In the present formulation, solving the multi-objective optimization problem typically suggests the determination of a set of Pareto optimal solutions.

Overall, the novelty of the proposed framework lies in that fact that it appears to be highly efficient for performing stochastic design optimization, reducing significantly the computational burden for this task. Specifically, the recently developed approximate nonlinear stochastic dynamics technique is appropriately tailored and incorporated in a robust performance-based framework for addressing the so called life-cycle cost stochastic design optimization problem; thus, circumventing computationally intensive Monte Carlo simulations that are ordinarily utilized in the literature so far. Further, an additional important feature relates to the utilization of the expected value of the life-cycle cost. In this manner, the contributions of all structural components are considered in the formulation herein, in contrast to the commonly adopted in the literature consideration of the most critical component contribution only.

2 NONLINEAR SYSTEM STOCHASTIC RESPONSE DETERMINATION

2.1 Statistical linearization treatment

In this section the most important elements of an approximate stochastic response determination technique developed by Kougioumtzoglou and Spanos [18] are included for completeness. Consider an n-degree-of-freedom nonlinear structural system governed by the equation

$$\mathbf{M\ddot{q}} + \mathbf{C\dot{q}} + \mathbf{Kq} + \mathbf{g(q,\dot{q})} = \mathbf{f}(t), \tag{1}$$

where $\ddot{\mathbf{q}}$, $\dot{\mathbf{q}}$ and $\mathbf{q}$ denote the response acceleration, velocity and displacement vectors, respectively, defined in relative coordinates; $\mathbf{M}$, $\mathbf{C}$ and $\mathbf{K}$ denote the $(n \times n)$ mass, damping and stiffness matrices, respectively; $\mathbf{g}(\mathbf{q}, \dot{\mathbf{q}})$ is assumed to be an arbitrary nonlinear $(n \times 1)$ vector function of the variables $\mathbf{q}$ and $\dot{\mathbf{q}}$; and $\mathbf{f}(t)^T = (f_1(t), f_2(t), \dots, f_n(t)$ is a $(n \times 1)$ zero mean, non-stationary stochastic vector process defined as $\mathbf{f}(t) = -\overline{\mathbf{M}}\boldsymbol{\gamma}\ddot{\alpha}_g(t)$, where $\boldsymbol{\gamma}$ is the unit column vector, $\ddot{\alpha}_g(t)$ is a stochastic non-stationary excitation process (e.g. earthquake excitation) and $\overline{\mathbf{M}}$ stands for the $(n \times n)$ mass matrix defined in absolute coordinates. Further, $\mathbf{f}(t)$ possesses an EPSD matrix $\mathbf{S_f}(\omega, t)$ of the form

$$\mathbf{S_f}(\omega, t) = \begin{bmatrix} m_1{}^2 S_{\ddot{\alpha}_g}(\omega, t) & 0 & \cdots & 0 \\ 0 & m_2{}^2 S_{\ddot{\alpha}_g}(\omega, t) & \cdots & 0 \\ \vdots & \ddots & \cdots & \vdots \\ 0 & 0 & \cdots & m_n{}^2 S_{\ddot{\alpha}_g}(\omega, t) \end{bmatrix}, \qquad (2)$$

while the non-stationary stochastic process $\mathbf{f}(t)$ is regarded to be a filtered stationary stochastic process [22]. Note that excitations exhibiting variability in both the intensity and the frequency content, and thus, possessing a non-separable EPSD can be considered as well.

In the following, a statistical linearization approach [1,2,3] is employed for determining the response EPSD matrix $\mathbf{S_q}(\omega, t)$. In this regard, a linearized version of Eq.(1) is given in the form

$$\mathbf{M}\ddot{\mathbf{q}} + (\mathbf{C} + \mathbf{C_{eq}})\dot{\mathbf{q}} + (\mathbf{K} + \mathbf{K_{eq}})\mathbf{q} = \mathbf{f}(t). \qquad (3)$$

Relying next on the standard assumption that the response processes are Gaussian, the time-dependent elements of the equivalent linear matrices $\mathbf{C_{eq}}$ and $\mathbf{K_{eq}}$ are given by the expressions

$$c_{i,j}^{eq} = E\left\{\frac{\partial g_i}{\partial \dot{q}_j}\right\}, \qquad (4)$$

and

$$k_{i,j}^{eq} = E\left\{\frac{\partial g_i}{\partial q_j}\right\}. \tag{5}$$

Next, omitting the convolution of the impulse response function matrix with the modulating matrix can lead to substantial reduction of computational effort, especially for the case of MDOF systems [23,24]. In this manner, the response EPSD matrix $\mathbf{S_q}(\omega, t)$ for the linearized system of Eq.(3) is given by

$$\mathbf{S_q}(\omega, t) = \mathbf{H}(\omega)\mathbf{S_f}(\omega, t)\mathbf{H^{T*}}(\omega). \tag{6}$$

where $\mathbf{H}(\omega)$ is the frequency response function (FRF) matrix defined as

$$\mathbf{H}(\omega) = \left(-\omega^2\mathbf{M} + i\omega(\mathbf{C} + \mathbf{C_{eq}}) + (\mathbf{K} + \mathbf{K_{eq}})\right)^{-1}. \tag{7}$$

Note that Eq.(6) can be regarded as a quasi-stationary approximate relationship which, in general, yields satisfactory accuracy in cases of relatively stiff systems [23,24]. Considering next Eqs.(2) and (6) yields the time-dependent variance of the response displacement and velocity for the i-th degree of freedom

$$\sigma_{q_i}^2(t) = \int_{-\infty}^{\infty}(|H_{i1}(\omega)|^2 m_1{}^2 + \cdots + |H_{in}(\omega)|^2 m_n{}^2)\, S_{\ddot{\alpha}_g}(\omega, t)d\omega, \tag{8}$$

and

$$\sigma_{\dot{q}_i}^2(t) = \int_{-\infty}^{\infty}\omega^2(|H_{i1}(\omega)|^2 m_1{}^2 + \cdots + |H_{in}(\omega)|^2 m_n{}^2)\, S_{\ddot{\alpha}_g}(\omega, t)d\omega. \tag{9}$$

Eqs.(8) and (9) hold true in the approximate quasi-stationary sense delineated earlier. Clearly, Eq.(6) can be used in conjunction with Eqs.(4-5) and (7-9) to form a nonlinear system of algebraic equations to be solved for determining the MDOF system response covariance matrix at a low computational cost [18]; thus, circumventing computationally intensive Monte Carlo simulations.

2.2 Dimension reduction approach

Following next the dimension reduction/decoupling approach developed in [18], an auxiliary effective linear time-variant (LTV) oscillator corresponding to the i-th DOF can be defined as

$$\ddot{q}_i + \beta_{aux,i}(t)\dot{q}_i + \omega_{aux,i}^2(t)q_i = f_i(t), \quad i = 1, \dots, n_{dof}, \tag{10}$$

where the time-varying equivalent stiffness $\omega_{aux,i}^2(t)$ and damping $\beta_{aux,i}(t)$ elements can be determined by equating the variances of the response displacement and velocity expressed utilizing the quasi-stationary FRF of Eq.(10) with the corresponding ones determined via Eqs.(8-9); this yields

$$\sigma_{q_i}^2(t) = \int_{-\infty}^{\infty} \left(\frac{1}{(\omega_{aux,i}^2(t) - \omega^2)^2 + (\beta_{aux,i}(t)\omega)^2} \right) m_i^2 S_{\ddot{a}_g}(\omega, t) d\omega, \tag{11}$$

and

$$\sigma_{\dot{q}_i}^2(t) = \int_{-\infty}^{\infty} \omega^2 \left(\frac{1}{(\omega_{aux,i}^2(t) - \omega^2)^2 + (\beta_{aux,i}(t)\omega)^2} \right) m_i^2 S_{\ddot{a}_g}(\omega, t) d\omega. \tag{12}$$

Clearly, Eqs.(11) and (12) constitute a nonlinear system of two algebraic equations to be solved for the unknowns $\omega_{aux,i}^2(t)$ and $\beta_{aux,i}(t)$. Further, relying primarily on the assumption of light damping, a stochastic averaging technique is applied for casting the second-order stochastic differential equation (SDE) of Eq.(10) into a first-order SDE [25,26] governing the evolution in time of the response amplitude process $\alpha_i(t)$ defined as

$$\alpha_i^2(t) = q_i^2(t) + \left(\frac{\dot{q}_i(t)}{\omega_{aux,i}(t)} \right)^2. \tag{13}$$

Furthermore, associated with the above-mentioned first-order SDE is the Fokker-Planck partial differential equation governing the evolution of the non-stationary response amplitude PDF

$p(\alpha_i, t)$ corresponding to the i-th degree of freedom. Next, the system non-stationary response amplitude α_i is assumed to follow a time-dependent Rayleigh distribution of the form [18,27]

$$p(\alpha_i, t) = \frac{\alpha_i}{\theta_i(t)} \exp\left(-\frac{\alpha_i{}^2}{2\theta_i(t)}\right). \tag{14}$$

Substituting Eq.(14) into the Fokker-Planck partial differential equation, yields a first-order ordinary differential equation of the form

$$\dot{\theta}_i(t) = -\beta_{aux,i}(t)\theta_i(t) + \frac{\pi S_f\left(\omega_{aux,i}(t), t\right)}{\omega_{aux,i}^2(t)}, \tag{15}$$

to be solved via standard numerical integration schemes such as the Runge-Kutta; see also [26-28]. Overall, it can be readily seen that the approximate analytical technique presented in section 2 not only determines the original MDOF system response amplitude PDF $p(\alpha_i, t)$ for each and every DOF in an efficient manner by circumventing computationally demanding MC simulations, but also decouples the original system providing with effective time-varying stiffness and damping elements corresponding to the i-th DOF. The latter feature is especially important for a number of reasons such as determining peak system response estimates based on design spectrum compatible excitation power spectra [29], tracking and avoiding moving resonance phenomena [30], and developing efficient approximate techniques for determining nonlinear system survival probabilities and first-passage PDFs [31,32].

Further, the herein considered damage states are expressed in terms of the inter-story drift ratio (IDR) that is defined as the difference of the horizontal displacements between two successive stories, normalized by the inter-story height h. Considering in the ensuing analysis the IDR amplitude $A_i(t)$, a direct transformation [33] of the response amplitude PDF $p(\alpha_i, t)$ yields the non-stationary IDR amplitude PDF in the form

$$p(A_i, t) = h^2 \frac{A_i}{\theta_i(t)} \exp\left(-\frac{h^2 A_i^2}{2\theta_i(t)}\right). \tag{16}$$

Further, of particular interest from a reliability assessment perspective is the time instant where the IDR amplitude reaches its most critical value, i.e. $p_{cr}(A_i) = p(A_i, t = t_{cr})$. In the following, this is assumed to be the time where $\theta_i(t)$ reaches its peak value, and thus, the PDF of Eq.(16) takes its most broad-band form yielding higher failure probabilities. Specifically, the failure probability P_i defined as the probability of exceeding various levels of damage δ_{ds} conditioned upon the peak ground acceleration (PGA), is expressed as

$$P_i[A_i(t) \geq \delta_{ds} = \delta | PGA = \alpha_{pga}] = 1 - \int_0^\delta p_{cr}\left(A_i(t) | PGA = \alpha_{pga}\right) dA \tag{17}$$

Considering Eq.(16), and integrating analytically Eq.(17) yields

$$P_i[A_i(t) \geq \delta_{ds} = \delta | PGA = \alpha_{pga}] = \exp\left(-\frac{h^2 \delta^2}{2\theta_i(t)}\right). \tag{18}$$

It is deemed appropriate to note that in the herein proposed framework, only failure definitions of the form of Eq.(18) are considered, whereas incorporation of first-passage [31,32,34] kind failure criteria is identified as a topic of potential future work.

3 SEISMIC LIFE-CYCLE COST EVALUATION

The PBEE methodology serves as a potent stochastic framework for assessing the performance of engineering structural systems subject to various hazards via an appropriately defined decision variable. Following a standard PBEE framework, as proposed by the Pacific Earthquake Engineering Research (PEER) center [35,36], the evaluation of a decision variable typically depends on a number of analysis components such as (i) stochastic hazard analysis treating the uncertainty in the seismic input intensity measures (IMs); the seismic hazard is usually described

by the annual probabilities of exceeding various levels of IMs, (ii) stochastic structural analysis associated with the uncertainty of the engineering demand parameter (EDP) used to monitor the structural response conditional on the IMs; the IDR is a commonly selected EDP for building structures, (iii) stochastic damage analysis relating the EDPs to damage states, which in turn describe the generated damage, and (iv) stochastic loss analysis reflecting the effect of the underlying uncertainties on a quantifiable decision variable.

The uncertainty in seismic ground motions is normally described in terms of the probability distribution of a seismic intensity measure, such as the peak ground acceleration (PGA). In this regard, the seismic hazard is presented as a mean seismic hazard curve $H(\alpha_{pga})$, which provides the annual probability of exceeding specified levels of PGA [37]; that is,

$$H(\alpha_{pga}) = P[PGA \geq \alpha_{pga}]. \tag{19}$$

In various PBEE studies [9,10] as well as in the ensuing analysis, discrete damage states are considered. The non-stationary IDR amplitudes $A_i(t)$ serve as global EDPs while the employed relationship between the EDP and the damage states, provided herein for illustration purposes, is based on the work by Ghobarah [38] related to ductile reinforced concrete (RC) moment resisting frames (see Table. 1). Note that IDR constitutes one of the most reliable measures of structural damage due to its close relationship to plastic rotation demands for individual beam-column connection assemblies. Typically, the damage states for reliability analysis purposes are defined in terms of the overall inelastic deformation or the maximum inter-story drift of the structural system [4].

Damage State	Inter-Story Drift (%)	Cost (% C_{in})
(I)-None	$0.0 \leq IDR_{Max} < 0.1$	0
(II)-Slight	$0.1 \leq IDR_{Max} < 0.2$	0.5
(III)-Light	$0.2 \leq IDR_{Max} < 0.4$	5
(IV)-Moderate	$0.4 \leq IDR_{Max} < 1.0$	20
(V)-Heavy	$1.0 \leq IDR_{Max} < 1.8$	45
(VI)-Major	$1.8 \leq IDR_{Max} < 3.0$	80
(VII)-Destroyed	$3.0 \leq IDR_{Max}$	100

Table 1. Damage states, Inter-story drift limits and associated costs.

Further, the seismic fragility curves serving as a quantitative tool of the structure vulnerability are evaluated for various damage levels. Specifically, the seismic fragility curves are efficiently determined by simply integrating the critical non-stationary response IDR amplitude PDF $p_{cr}(A_i)$ for the time instant t_{cr}; see Eqs.(16-17). In this regard, the probability of the i–th DOF exceeding various levels of damage given a specified PGA value, i.e. $P_i[A_i(t) \geq \delta_{ds} = \delta | PGA = \alpha_{pga}]$, can be efficiently computed via Eq.(18).

Notably, the fragility curves corresponding to each and every DOF for various damage levels are determined at a minimum computational cost via Eq.(18). Next, considering the i-th DOF of the MDOF system, the annual probability of exceeding a given state of damage can be defined as

$$P_{i,a} = \int P_i[A_i(t) \geq \delta_{ds} = \delta | PGA = \alpha_{pga}] \left| \frac{dH(\alpha_{pga})}{d\alpha_{pga}} \right| d\alpha_{pga}. \tag{20}$$

In the current study, the earthquake occurrence is assumed to follow a Poisson process [39]. Further, the expected value of the life-cycle cost (LCC) due to seismic hazard can be expressed in the form

$$E[LCC(A_i(\mathbf{x}, \mathbf{t}))] = \frac{1}{\lambda T_d}(1 - \exp(-\lambda T_d)) \times \ldots$$

$$\sum_{i=1}^{n_{dof}} \sum_{m=1}^{n_{ds}} \left(-C_m \left[\ln \left(1 - P_{i,T_d}(A_i(t) > \delta_m) \right) - \ln \left(1 - P_{i,T_d}(A_i(t) > \delta_{m+1}) \right) \right] \right), \tag{21}$$

where n_{ds} is the total number of damage states considered; n_{dof} is the number of degrees of freedom of the MDOF system, λ is a constant discount rate/year, T_d is the design life of the structure, C_m is the cost associated with the m-th damage state, given in Table.1 as a percentage of the initial cost; P_{i,T_d} refers to the i-th DOF and represents the T_d-year probability of exceeding the m-th damage state given by the expression

$$P_{i,T_d} = 1 - \exp\left(-P_{i,a} T_d \right). \tag{22}$$

Furthermore, it is assumed that the structure is restored to its initial undamaged state after each earthquake occurrence and losses due to fatalities and building downtime are ignored.

The fact that this study involves damage costs makes it important to consider all degrees of freedom, as opposed to only the critical component that is usually employed in PBEE studies [4,9,10]. Considering cases where the roof drift is employed as an EDP, the corresponding damage analysis cannot account for the distribution of damage along the height of the structure, or take into account soft stories phenomena [38]. Further, in many studies in the literature, the adoption of the maximum value of the induced inter-story drifts as an EDP leads to a subsequent stochastic damage analysis based on information corresponding to a specific story only. Thus, information regarding the response behavior of the rest of the stories and their contribution to damage is disregarded.

Overall, in the herein proposed life-cycle cost formulation the expected value of the seismic losses given by Eq.(21) serves as the decision variable, whereas the attribute of considering n_{dof} EDPs is expected to better account for the system overall performance in the formulation of the

multi-objective optimization problem in the following section.

4   MULTI-OBJECTIVE DESIGN PROBLEM FORMULATION

In the field of structural system optimization, most often several conflicting objectives need to be treated simultaneously. In this regard, a multi-objective optimization problem is formulated yielding a compromise between various objective functions. A general stochastic multi-objective optimization formulation for the determination of a vector $\mathbf{x}$ of design variables to minimize a vector of objective functions takes the form

$$\min_{\mathbf{x} \in D} \mathbf{F}(\mathbf{x}), \tag{23}$$

where

$$\mathbf{F}(\mathbf{x}) = \left[f_z^{ind}(\mathbf{x}) \right] = \left[f_1^{ind}(\mathbf{x}), \dots, f_{nobj}^{ind}(\mathbf{x}) \right], z = 1, \dots, n_{obj}$$

$$\mathbf{x} = \left[x_j \right] = \left[x_1, x_2, \dots x_{n_{dv}} \right]^T, j = 1, \dots n_{dv}, \mathbf{x} \in D, \tag{24}$$

subject to system response level constraints of the form

$$\mathbf{G}(\mathbf{x}) = \left[g_p^{ind}(\mathbf{x}) \right] = \left[g_1^{ind}(\mathbf{x}), \dots, g_{ncon}^{ind}(\mathbf{x}) \right] \leq 0, p = 1, \dots, n_{con}. \tag{25}$$

The superscript (ind) denotes the nature of the objective function or constraint which in turn is indicated by the subscripts (obj) and (con) respectively. In the case of a stochastic objective function $m_{f_z}^{stoch}(\mathbf{x})$ and $\sigma_{f_z}^{stoch}(\mathbf{x})$ are employed. $m_{f_z}^{stoch}(\mathbf{x})$ and $\sigma_{f_z}^{stoch}(\mathbf{x})$ are the maximum over time non-stationary values of the mean and standard deviation of the objective function f_z respectively, evaluated at the design variables vector $\mathbf{x}$; $f_z^{det}(\mathbf{x})$ is a deterministic objective function evaluated at the design variables vector $\mathbf{x}$; in case of a stochastic response constraint, $m_{g_p}^{stoch}(\mathbf{x})$, $\mu_{g_p}^{stoch}(\mathbf{x})$ and $\sigma_{g_p}^{stoch}(\mathbf{x})$ stand for the maximum over time non-stationary values of the mean, mode and standard deviation of the response function g_p respectively, evaluated at the

design variables vector $\mathbf{x}$; $g_p^{det}(\mathbf{x})$ is a deterministic response level constraint evaluated at the design variables vector $\mathbf{x}$; and $\mathbf{G}(\mathbf{x})$ is the vector of the constraint functions of the optimization problem under consideration. D is a given set that contains the boundary constraints for the vector of design variables $\mathbf{x}$.

Further, a weighted linear combination of the aforementioned quantities, which is the case in most practical applications [21], is considered in the herein work as well. In this regard, a single parameterized objective function $\mathbf{F}(\mathbf{x})$ under several optimization runs with different parameter settings is responsible for the generation of the Pareto optimal set [40], i.e.

$$\mathbf{F}(\mathbf{x}) = \sum_{k=1}^{n_{obj}^{stoch}} \left(\frac{w_{\mu,\kappa}}{s_{\mu,\kappa}} m_{f_k}^{stoch}(\mathbf{x}) + \frac{w_{\sigma,\kappa}}{s_{\sigma,\kappa}} \sigma_{f_k}^{stoch}(\mathbf{x}) \right) + \sum_{n=1}^{n_{obj}^{det}} \left(\frac{w_n}{s_n} f_n^{det}(\mathbf{x}) \right), \qquad (26)$$

where $w_{\mu,\kappa}$, $w_{\sigma,\kappa}$ are weights and $s_{\mu,\kappa}$, $s_{\sigma,\kappa}$ are scale factors for the mean and standard deviation of the stochastic objective components $f_k^{stoch}(\mathbf{x})$, $k = 1, \dots, n_{obj}^{stoch}$; w_n and s_n are the weight and scale factor of the deterministic objective components $f_n^{det}(\mathbf{x})$, $n = 1, \dots, n_{obj}^{det}$. Regarding the weighting factors w the following normalization is employed

$$\sum_{z=1}^{n_{obj}} w_z = 1. \qquad (27)$$

The weighting factors can be adjusted appropriately, according to the importance of each objective and therefore the trade-off between the objectives can be readily studied. Any combination of the weighting factors corresponds to a single Pareto optimal solution [9,10,21]. Thus, by performing a set of optimization processes utilizing various weighting factors combinations it is possible to generate the full set of the Pareto optimal solutions.

Since the generation of the Pareto optimal set involves performing a number of optimization

procedures, the selection of an optimization algorithm with considerable advantages specifically tailored to meet the characteristics of the herein problem formulation is of particular importance. Specifically, an outer loop that systematically varies the weighting factors of the parameterized objective function and an inner loop that features a standard genetic algorithm based optimization process are utilized for solving the multi-objective optimization problem. Regarding genetic algorithms, they belong to the class of Evolutionary algorithms and they appear to be quite robust in the sense that they are less vulnerable to being trapped in local optima; and thus, more likely to obtain the global optimum for a non-convex constrained optimization problem [41].

5 NUMERICAL APPLICATION

5.1 Three-story Bouc-Wen hysteretic building structure

In this section, the proposed methodology is applied to a 3-story reinforced concrete building which is modeled as a nonlinear/hysteretic 3-DOF structural system subject to evolutionary stochastic earthquake excitations. All floors are assumed to be rigid and have a constant height equal to 3m, whereas the masses of the plates are considered to be constant for all floors with a value $m_{plate} = 3.5 \times 10^4$kg. A Young's modulus of $E = 30 \times 10^9$Pa and mass density of $\rho = 2,5 \times 10^3$kg/m^3 are considered herein. Columns' cross-section dimensions for a given floor are assumed to be equal, and thus, the vector of design variables **x** has one component for every story, i.e. the width of the cross-section.
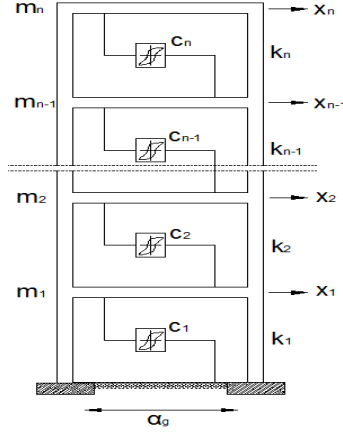
Figure 1. A general nonlinear/hysteretic MDOF structural system.

The nonlinearity is assumed to be in the form of the Bouc-Wen hysteretic model [42]. In this regard, considering inter-story drifts q_i ($q_i = x_i - x_{i-1}$, $i = 1, \ldots, n_{dof}$) as well as the additional states z_i, the 3-DOF nonlinear structural system is governed by Eq.(1) where

$$\mathbf{q}^T = (q_1 \; q_2 \; q_3 \; z_1 \; z_2 \; z_3) \tag{28}$$

$$\mathbf{M} = \begin{bmatrix} \mathbf{M_{11}} & \mathbf{M_{12}} \\ \mathbf{M_{21}} & \mathbf{M_{22}} \end{bmatrix}, \tag{29}$$

where

$$\mathbf{M_{11}} = \begin{bmatrix} m_1 & 0 & 0 \\ m_2 & m_2 & 0 \\ m_3 & m_3 & m_3 \end{bmatrix}, \tag{30}$$

and

$$\mathbf{M_{12}} = \mathbf{M_{21}} = \mathbf{M_{22}} = \begin{bmatrix} 0 & 0 & 0 \\ 0 & 0 & 0 \\ 0 & 0 & 0 \end{bmatrix}. \tag{31}$$

$$\mathbf{K} = \begin{bmatrix} \mathbf{K_{11}} & \mathbf{K_{12}} \\ \mathbf{K_{21}} & \mathbf{K_{22}} \end{bmatrix}, \tag{32}$$

where

$$\mathbf{K_{11}} = \begin{bmatrix} ak_1 & -ak_2 & 0 \\ 0 & ak_2 & -ak_3 \\ 0 & 0 & ak_3 \end{bmatrix}, \tag{33}$$

$$\mathbf{K_{12}} = \begin{bmatrix} (1-a)k_1 & -(1-a)k_2 & 0 \\ 0 & (1-a)k_2 & -(1-a)k_3 \\ 0 & 0 & (1-a)k_3 \end{bmatrix}, \tag{34}$$

and

$$\mathbf{K_{21}} = \mathbf{K_{22}} = \begin{bmatrix} 0 & 0 & 0 \\ 0 & 0 & 0 \\ 0 & 0 & 0 \end{bmatrix}. \tag{35}$$

In Eqs.(33-34) the parameter a stands for the rigidity ratio and can be viewed as a form of post-yield to pre-yield stiffness ratio ($a = 1$ corresponds to the linear system). Further, the damping matrix of the structural system $\mathbf{C}$ takes the form

$$\mathbf{C} = \begin{bmatrix} \mathbf{C_{11}} & \mathbf{C_{12}} \\ \mathbf{C_{21}} & \mathbf{C_{22}} \end{bmatrix}, \tag{36}$$

where

$$\mathbf{C_{11}} = c_0 \cdot \mathbf{K_{11}}, \tag{37}$$

$$\mathbf{C_{12}} = \mathbf{C_{21}} = \begin{bmatrix} 0 & 0 & 0 \\ 0 & 0 & 0 \\ 0 & 0 & 0 \end{bmatrix}, \tag{38}$$

and

$$\mathbf{C_{22}} = \begin{bmatrix} 1 & 0 & 0 \\ 0 & 1 & 0 \\ 0 & 0 & 1 \end{bmatrix}. \tag{39}$$

In Eq.(37) c_0 is taken equal to 0.2×10^{-2}. Next, the loading vector becomes

$$\mathbf{F}(t)^T = (f_1(t) \ f_2(t) \ f_3(t) \ 0 \ 0 \ 0), \tag{40}$$

and

$$\mathbf{g}(\mathbf{q}, \dot{\mathbf{q}})^{\mathbf{T}} = \left(0\ 0\ 0\ -g_1(\dot{q}_1, z_1)\ -g_2(\dot{q}_2, z_2)\ -g_3(\dot{q}_3, z_3)\right). \tag{41}$$

In the Bouc-Wen model the additional state z_i is associated with the inter-story drift q_i via the nonlinear differential equation

$$\dot{z}_i = g_i(\dot{q}_i, z_i), \tag{42}$$

where

$$g_i(\dot{q}_i, z_i) = -\gamma|\dot{q}_i|z_i|z_i|^{n-1} - \beta\dot{q}_i|z_i|^n + A\dot{q}_i. \tag{43}$$

In Eq.(43) the parameters γ, β, A and n are capable of representing a wide range of hysteresis loops [42]. The values $a = 0.15$, $\beta = \gamma = 0.5$, $n = 1$ and $A = 1$ are considered herein. Next, the equivalent linear matrices take the form [1,3]

$$\mathbf{C_{eq}} = \begin{bmatrix} \mathbf{C_{eq11}} & \mathbf{C_{eq12}} \\ \mathbf{C_{eq21}} & \mathbf{C_{eq22}} \end{bmatrix}, \tag{44}$$

where

$$\mathbf{C_{eq11}} = \mathbf{C_{eq12}} = \mathbf{C_{eq22}} = \begin{bmatrix} 0 & 0 & 0 \\ 0 & 0 & 0 \\ 0 & 0 & 0 \end{bmatrix}, \tag{45}$$

and

$$\mathbf{C_{eq21}} = \begin{bmatrix} c_{eq1} & 0 & 0 \\ 0 & c_{eq2} & 0 \\ 0 & 0 & c_{eq3} \end{bmatrix}. \tag{46}$$

$$\mathbf{K_{eq}} = \begin{bmatrix} \mathbf{K_{eq11}} & \mathbf{K_{eq12}} \\ \mathbf{K_{eq21}} & \mathbf{K_{eq22}} \end{bmatrix}, \tag{47}$$

where

$$\mathbf{K_{eq11}} = \mathbf{K_{eq12}} = \mathbf{K_{eq21}} = \begin{bmatrix} 0 & 0 & 0 \\ 0 & 0 & 0 \\ 0 & 0 & 0 \end{bmatrix}, \tag{48}$$

and

$$\mathbf{K_{eq22}} = \begin{bmatrix} k_{eq1} & 0 & 0 \\ 0 & k_{eq2} & 0 \\ 0 & 0 & k_{eq3} \end{bmatrix}. \tag{49}$$

Furthermore, the elements c_{eq_i} and k_{eq_i} are given by the expressions

$$c_{eq_i} = \sqrt{\frac{2}{\pi}} \left[\gamma \frac{E(\dot{q}_i z_i)}{\sqrt{E(\dot{q}_i{}^2)}} + \beta \sqrt{E(z_i{}^2)} \right] - A, \tag{50}$$

and

$$k_{eq_i} = \sqrt{\frac{2}{\pi}} \left[\gamma \sqrt{E(\dot{q}_i{}^2)} + \beta \frac{E(\dot{q}_i z_i)}{\sqrt{E(z_i{}^2)}} \right], \tag{51}$$

respectively. Regarding the excitation EPSD $S_{\ddot{\alpha}_g}(\omega, t)$, it is assumed to have the separable form

$$S_{\ddot{\alpha}_g}(\omega, t) = |g(t)|^2 S_{CP}(\omega), \tag{52}$$

where $S_{CP}(\omega)$ represents a stationary process power spectral density and $g(t)$ denotes a time-modulating function. The envelope function $g(t)$ is given by

$$g(t) = k\left(e^{-b_1 t} - e^{-b_2 t}\right), \tag{53}$$

where $b_1 = 0.1$ and $b_2 = 0.3$; k is a normalization constant so that $g(t)_{max} = 1$, thus Eq.(52) has a uniform modulation. The widely used Kanai-Tajimi spectrum appropriately modified by Clough and Penzien [43] is considered for $S_{CP}(\omega)$; that is,

$$S_{CP}(\omega) = S_0 \frac{(\omega/\omega_f)^4}{(1-(\omega/\omega_f)^2)^2 + 4\xi_f^2(\omega/\omega_f)^2} \frac{\omega_g^4 + 4(\xi_g)^2\omega_g^2\omega^2}{(\omega_g^2 - \omega^2)^2 + 4\xi_g^2\omega_g^2\omega^2} \qquad (54)$$

where S_0 is the amplitude of the bedrock excitation spectrum, modeled as a white noise process; ξ_g and ω_g are the damping factor of the soil and the fundamental natural frequency, respectively; and ξ_f and ω_f are parameters describing the Clough-Penzien filter. The parameters values chosen are $\xi_g = 0.7, \omega_g = 2$ rad/s, $\xi_f = 0.6, \omega_f = 12.5$ rad/s. At this point, it is deemed appropriate to note that the proposed framework can readily address in a straightforward manner also cases where the excitation input is of the non-separable kind. Next, the duration of the earthquake excitation t_o is taken equal to 20s. Note that in the ensuing analysis the following definition for the α_{pga} is adopted; i.e.,

$$\alpha_{pga} = E\left[\max(|\ddot{\alpha}_g(t)|)\right], \quad 0 \le t \le t_o \qquad (55)$$

Thus, to provide with a mapping between the α_{pga} and the modulated Clough-Penzien excitation spectrum intensity factor S_0, several MCS are conducted for various S_0 values via the spectral representation approach [44]. For each ensemble of excitation realizations Eq.(55) is applied for determining the value α_{pga} that corresponds to the given S_0. In this manner, repeating this process for various values of S_0 the relationship $S_0(\alpha_{pga})$ depicted in Fig.(2) is obtained.
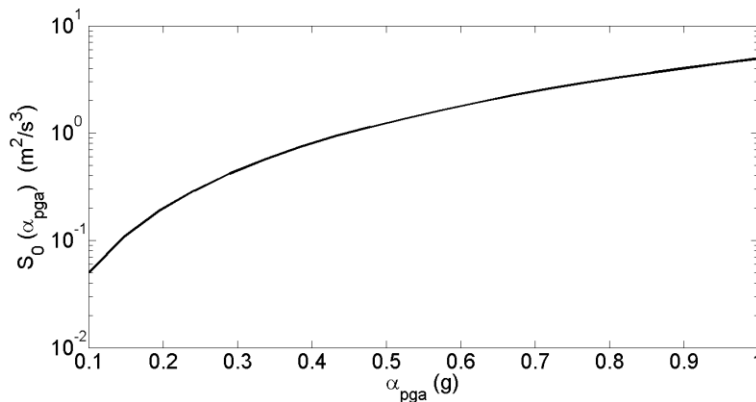
Figure 2. Mapping between the $S_0(\alpha_{pga})$ of the excitation spectrum and α_{pga}.

In Fig.(3), the EPSD of $S_{\ddot{\alpha}_g}(\omega, t)$ is plotted for $S_0 = 0.5692 \text{ m}^2/\text{s}^3$ which corresponds to an acceleration of the earthquake input α_{pga} equal to $0.34g$ according to the definition of Eq.(55).
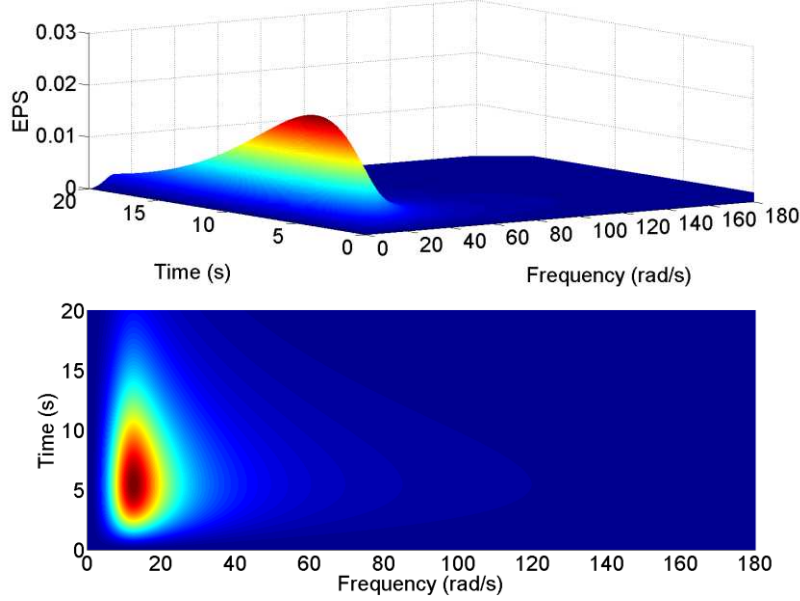

Figure 3. Clough-Penzien Evolutionary Power Spectral Density $S_{\ddot{\alpha}_g}(\omega, t)$.

Note that the herein utilized Clough-Penzien spectrum has been widely used in earthquake engineering applications, also as an excitation power spectrum model compatible with the seismic design spectrum [29]. Next, the seismic hazard curve of Eq.(19) is expressed in the approximate form used in [37], i.e.,

$$H(\alpha_{pga}) = P[PGA \geq \alpha_{pga}] = k_0 \times \alpha_{pga}^{-k_1}, \tag{56}$$

where $k_0 = 6.734 \times 10^{-5}$ and $k_1 = 2.857$. Note that when dealing with the evaluation of the expected value of LCC (see Eq.(21)), and for the purpose of taking into account all possible earthquake scenarios a structure is anticipated to encounter during its lifetime, all seismic events with acceleration input α_{pga} values between 0.1 and 1g are considered. In this setting, a wide range

of imposed seismic inputs α_{pga} is regarded while neglecting those with ground acceleration less than 0.1g that are not expected to cause significant damage to the structure.

Further, approximate technique based data are compared with pertinent Monte Carlo simulation data utilizing 10,000 realizations. Specifically, excitation realizations compatible with the EPSD of Eq.(54) are generated based on the spectral representation technique [44]. Next, the nonlinear equation of motion (Eq.(1)) is numerically integrated via a standard fourth order Runge-Kutta scheme, and finally, system response statistics are obtained based on the ensemble of the response realizations. In this regard, to provide with an indicative order of magnitude for the computational cost involved, utilizing a laptop computer with standard configurations, the technique based on the Rayleigh approximation requires 4–5 min, whereas the MCS based system response EPSD estimation (10,000 time histories) requires 12–13 h, depending on the specific application. Indicatively, in Figs.(4a) and (4b), the non-stationary response IDR amplitude PDFs determined via the approximate technique are compared with corresponding MCS data for an initial design variables vector $\mathbf{x}^{in} = [0.30\text{m}, 0.25\text{m}, 0.20\text{m}]^{T}$. The seismic excitation intensity level S_0 is selected to yield a α_{pga} value equal to 0.34g; see Fig.(3). Note in passing that it can be argued that even in cases where the system response PDF deviates considerably from the Gaussian one, the magnitude of this discrepancy is reduced when referring to system response amplitude PDF. It can be readily seen that the proposed approximate stochastic dynamics technique demonstrates a satisfactory degree of accuracy.
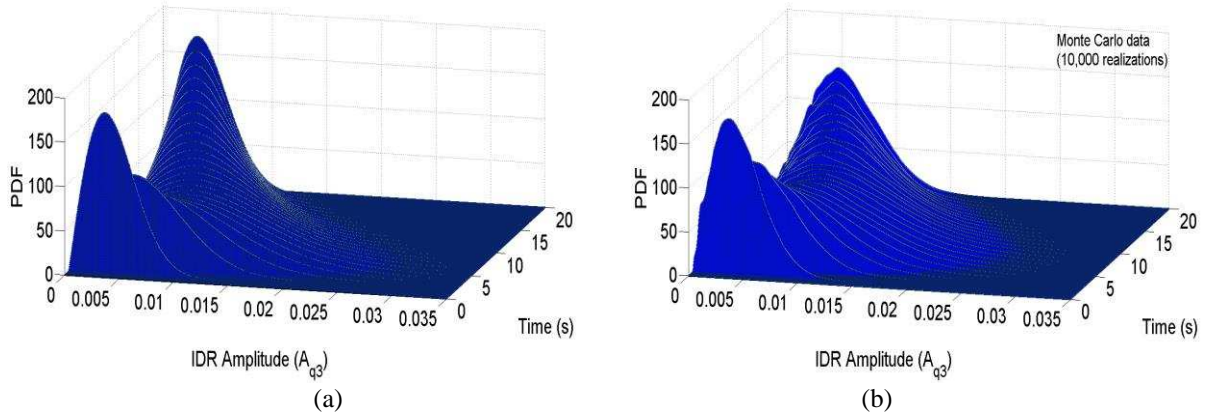
(a)   (b)

Figure 4. Non-stationary response IDR amplitude PDFs corresponding to the third story of the hysteretic MDOF structural system (a) via the analytical approach (b) Monte Carlo data (10,000 realizations).

Further, in Figs. (5a) and (5b) the most critical response IDR amplitude PDFs $p_{cr}(A_i) = p(A_i, t = t_{cr})$ are plotted for two distinct $\mathbf{x}$ design variables values and compared with MCS data demonstrating a reasonable degree of accuracy.
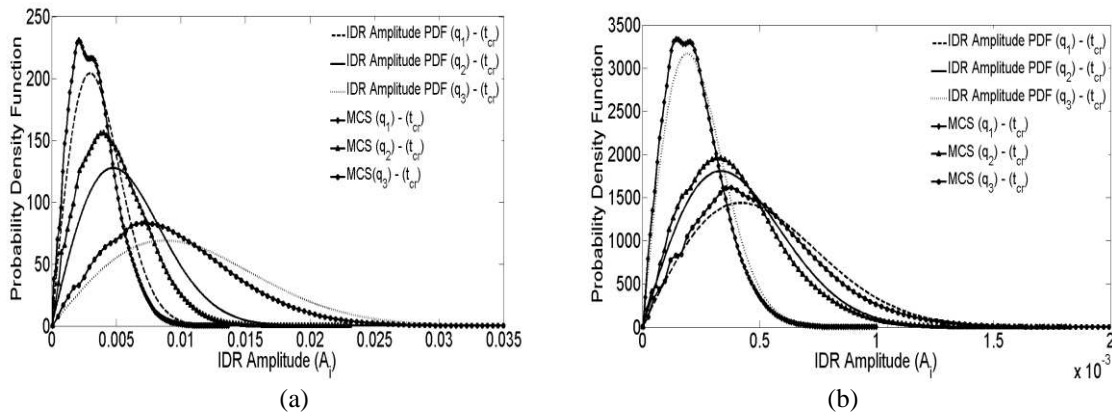

(a)   (b)

Figure 5. Non-stationary response IDR amplitude PDF of every story of the hysteretic MDOF system; comparison with MCS (a) $\mathbf{x}^{in} = [0.30m, 0.25m, 0.20m]^T$ and (b) $\mathbf{x}^{ub} = [0.55m, 0.55m, 0.55m]^T$.

Comparing Figs.(5a) and (5b) it can be readily seen that a slightly higher level of accuracy is observed in Fig.(5b). To explain this, note that in Fig.(5b) the chosen design vector $\mathbf{x}^{ub}$ which corresponds to an upper design bound with value $[0.55m, 0.55m, 0.55m]^T$ yields a relatively

stiffer structure than the one depicted in Fig.(5a), where $\mathbf{x}^{\text{in}} = [0.30\text{m}, 0.25\text{m}, 0.20\text{m}]^{\text{T}}$. As pointed out in section 2 and explained in detail in [18,23,24] the approximation induced by considering Eq.(6) implies a relatively lower level of accuracy for "softer" systems. Nevertheless, as shown in Fig.(5a), even in cases where the technique deviates slightly from the exact value, it still provides with conservative estimates; thus, rendering itself well-suited for structural design applications. Clearly, the determination of response IDR amplitude PDFs efficiently is a key factor for the subsequent fragility and loss analysis as well as for conducting the optimization procedure of the proposed PBEE framework.

Next, in Fig. (6) the fragility curves for each damage state are indicatively plotted for one story of the MDOF structural system; see Table 1.
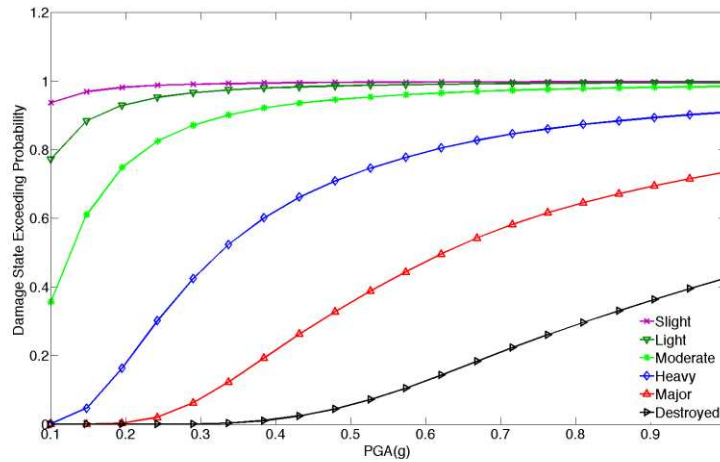

Figure 6. Fragility curves for the third story of the hysteretic MDOF structural system considering each damage state ($\mathbf{x}^{\text{in}} = [0.30\text{m}, 0.25\text{m}, 0.20\text{m}]^{\text{T}}$).

5.2 Multi-objective Optimal Designs – Pareto Front Curves

The objective function is defined as a weighted linear combination of the initial cost function and of the expected value of the life-cycle cost (LCC). Further, the response of the structural system is constrained in terms of the modes (i.e. most probable values) of the non-stationary response IDR amplitude PDFs of every DOF of the hysteretic MDOF system. The design variables

are the dimensions of the square cross-section of the column elements. Columns' cross-section dimensions for a given floor are assumed to be equal, and thus the vector of design variables $\mathbf{x}$ has three components, one for every story. Next, assuming an initial design $\mathbf{x}^{in} = [0.30m, 0.25m, 0.20m]^T$ and boundary constraints $x_i^{in} \leq x_i \leq x_i^{ub}$, $i = 1, \dots, n_{dof}$, where $\mathbf{x}^{ub} = [0.55m, 0.55m, 0.55m]^T$ the optimization problem takes the form

$$\min_{\mathbf{x} \in D}(\mathbf{F}(\mathbf{x})) = \min_{\mathbf{x} \in D}(C_{in}, E[LCC(A_i(\mathbf{x}, \mathbf{t}))]), \tag{57}$$

where the conflicting sub-objectives are normalized appropriately (see section 4) under the stochastic constraints

$$\boldsymbol{\mu}_{\mathbf{o},\mathbf{i}}(S_o^*, \mathbf{x}, \mathbf{t}) = \frac{\sqrt{c_i(t)}}{h} \leq \boldsymbol{\delta}_{ds}^{Limit}, \tag{58}$$

and

$$\boldsymbol{\omega}_{aux,i}(S_o^*, \mathbf{x}, \mathbf{t})_{,max} \leq \boldsymbol{\omega}_{cr,L} \quad \text{or} \quad \boldsymbol{\omega}_{aux,i}(S_o^*, \mathbf{x}, \mathbf{t})_{,min} \geq \boldsymbol{\omega}_{cr,R} \tag{59}$$

and the deterministic constraint

$$x_i \geq x_{i+1}, \quad i = 1, \dots, n_{dof}. \tag{60}$$

In Eq.(57) $C_{in}(\mathbf{x})$ stands for the initial cost which is assumed to be directly proportional to the building structure weight; this includes the weight of the column elements plus the weight of the plates evaluated at the design variables vector $\mathbf{x}$; $E[LCC(A_i(\mathbf{x}, \mathbf{t}))]$ is the expected value of the life-cycle cost, evaluated at the design variables vector $\mathbf{x}$. In Eq.(58) $\boldsymbol{\mu}_{\mathbf{o},\mathbf{i}}(S_o^*, \mathbf{x}, \mathbf{t})$ is a vector of the modes of the non-stationary response IDR amplitude PDFs of every story of the hysteretic MDOF system for the whole duration t_o of the seismic excitation with intensity factor S_o^*, evaluated at the design variables vector $\mathbf{x}$. The structure design service life T_d is considered to be equal to fifty years while the discount ratio, λ, is taken to be equal to 3%. Regarding the stochastic constraints

of Eqs.(58) and (59) the critical excitation was selected to be the one with intensity factor S_o^* yielding an earthquake input α_{pga} equal to 0.34g; see Fig(3). The rationale behind this choice lies in the fact that the above chosen value for α_{pga} represents a relatively severe earthquake event which is characterized by a low annual probability of occurrence according to the selected seismic hazard curve; thus, highly appropriate for applying constraints considering safety issues [5,9]. In this setting, the imposed stochastic constraint of Eq.(58) ensures that the vector of the modes of the non-stationary response IDR amplitude PDFs of every story of the hysteretic structural system for the whole duration t_o of the seismic excitation with intensity factor S_o^* will not exceed a preselected limit δ_{ds}^{Limit} which is taken equal to 0.2% and corresponds to a specific damage state according to the defined IDR limits of Table 1.

Further, regarding the constraint of Eq.(59), it exploits the time-varying effective stiffness $\omega_{aux,i}^2(t)$ and damping $\beta_{aux,i}(t)$ elements, stemming from the efficient decoupling of the original n-DOF system of Eq.(1) into n SDOF LTV oscillators of the form of Eq.(10). This important feature of the technique is exploited in the proposed formulation in the constraint of Eq.(59) for avoiding "moving resonance" phenomena [30]. In this regard, it facilitates the optimization process to avoid unnecessary optimal design searching in areas where surely optimal designs do not exist. Specifically, considering the quasi-stationary treatment of the LTV oscillator in Eq.(11), it can be reasonably argued that the maximum response variance of the original MDOF system occurs when the excitation EPSD $S_{\ddot{\alpha}_g}(\omega, t)$ resonates with the LTV oscillator equivalent natural frequency $\omega_{aux,i}(t)$. Thus, to avoid this resonance phenomenon, the constraint of Eq.(59) is formulated so that $\omega_{aux,i}(t)$ is kept outside a critical range in the frequency domain $[\omega_{cr,L}, \omega_{cr,R}]$ where the excitation EPSD $S_{\ddot{\alpha}_g}(\omega, t)$ takes its largest values. In this regard, the expression

$$S_{\ddot{\alpha}_{g,L}}(\omega, t) \leq \varepsilon \times S_{\ddot{\alpha}_{g,P}}^{*}(\omega, t) \tag{61}$$

is adopted, where $S_{\ddot{\alpha}_{g,L}}(\omega, t)$ is a selected EPSD value given as a percentage ε of the peak EPSD value $S_{\ddot{\alpha}_{g,P}}^{*}(\omega, t)$ corresponding to the time instant where $|g(t)|^2$ takes its peak value; see Figs.(3), (7a) and (7b). In this application, ε was taken equal to 75%.
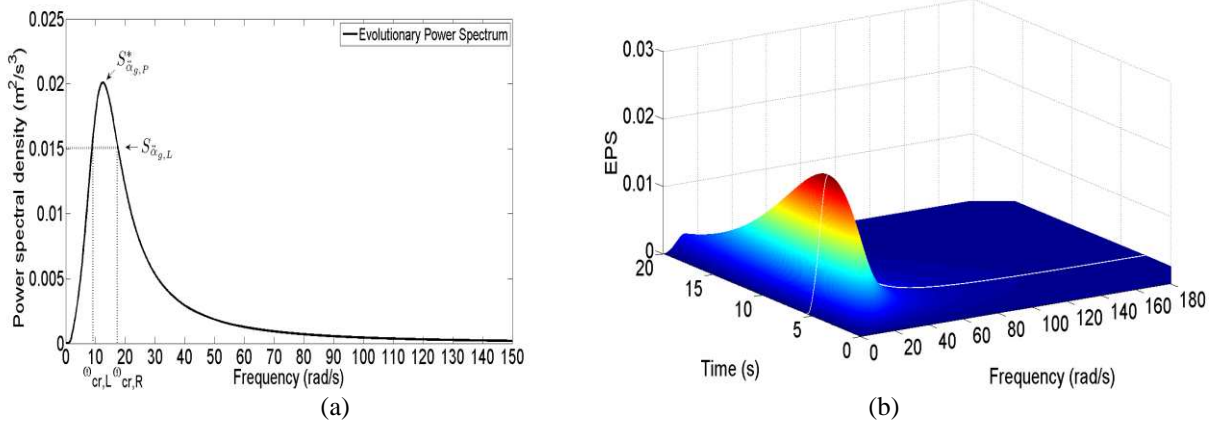

Figure 7. Depiction of the stochastic constraint for avoiding resonance phenomena.

Note that the deterministic constraints of Eq.(60) ensure that the optimization procedure will provide applicable design solutions from a practical viewpoint. Further, the expected value of the total cost, the initial cost and the expected value of the life-cycle cost are related according to the following expression [6]

$$E[C_{Total}(A_i(\mathbf{x}, \mathbf{t}))] = C_{in}(\mathbf{x}) + E[LCC(A_i(\mathbf{x}, \mathbf{t}))] \times C_{in}(\mathbf{x}). \tag{62}$$

The Pareto front curves obtained by compromise programming, utilizing the linear weighting method in a MATLAB's built-in genetic algorithm constraint optimization algorithm for both the expected value of the life-cycle cost and the total cost with respect to the initial cost are presented in Fig.(8).
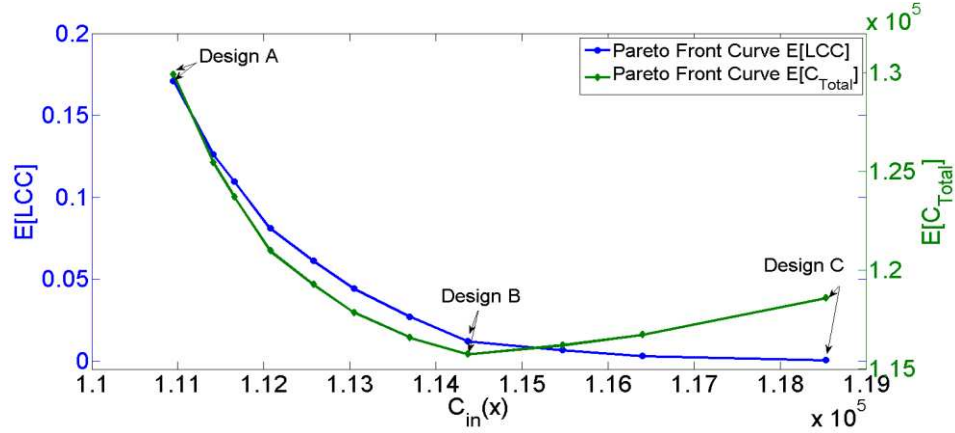
Figure 8. Pareto front curves for the expected values of LCC and Total cost.

Each solution of the Pareto front curves constitutes an applicable design configuration compromising the conflicting sub-objectives of the problem while respecting the imposed stochastic and deterministic constraints. Next, to highlight the flexibility of the proposed methodology, the compromise design solution exhibiting the lowest expected value of the total cost, as well as the ones corresponding to the two tails (Fig.(8)) are presented in Table 2.

Designs		$\mathbf{x}$(m)	$C_{in}(\mathbf{x})$	$E[LCC(A_i(\mathbf{x}, \mathbf{t}))]$	$E[C_{Total}(A_i(\mathbf{x}, \mathbf{t}))]$
Design A	1st	0.3892			
	2nd	0.3701	1.1095×10^5	17.1103×10^{-2}	1.2993×10^5
	3rd	0.3294			
Design B	1st	0.4750			
	2nd	0.4749	1.1415×10^5	1.1302×10^{-2}	1.1544×10^5
	3rd	0.3981			
Design C	1st	0.5492			
	2nd	0.5489	1.1853×10^5	5.5901×10^{-4}	1.1860×10^5
	3rd	0.5471			

Table 2. Pareto optimal designs configurations A, B and C.

Note that the tail designs (i.e. Designs A and C) correspond to the single-objective optimal designs where the building structure weight and the life-cycle cost were used as the objective functions respectively. Clearly, design configuration A is more susceptible to future seismic

excitations, thus it presents the highest expected value of life-cycle cost (Table 2). Further, considering the herein formulation of the multi-objective optimization problem, the Pareto optimal design B consists perhaps the most rational design configuration. However, the implementation of the Pareto technique allows the designer/analyst to possess a considerable amount of information for any compromise solution configuration, rather than being limited to a unique optimal solution. This is of particular importance for an educated decision-making analysis where the final optimal design will be the compromise solution that best balances the initial cost, the life-cycle cost, and the total cost according to the project stakeholders' perspective.

6   CONCLUDING REMARKS

In this paper, a performance-based multi-objective design optimization framework considering life-cycle cost has been developed for nonlinear/hysteretic multi-degree-of-freedom (MDOF) structural systems subject to evolutionary stochastic excitations.

In the core of the stochastic structural analysis component of the proposed framework lies an efficient approximate dimension reduction technique for determining the non-stationary system response amplitude probability density functions (PDFs) based on the concepts of statistical linearization and of stochastic averaging; thus, computationally intensive Monte Carlo simulations are circumvented. The important additional output of yielding time-varying effective stiffness $\omega_{aux,i}^2(t)$ and damping $\beta_{aux,i}(t)$ elements is sufficiently exploited through the proposed framework by introducing constraints for avoiding "moving resonance" phenomena. Note that excitations with arbitrary non-separable EPSD forms that exhibit strong variability in both the intensity and the frequency content can be readily accounted for through the presented framework.

In this regard, considering appropriately defined damage measures structural system related fragility curves for each story are determined at a low computational cost as well. Finally, the

structural system design optimization problem is formulated as a multi-objective one to be solved by a genetic algorithm based approach; thus, various compromise solutions are obtained providing the designer with enhanced flexibility regarding decision-making analysis. A building structure comprising the versatile Bouc-Wen (hysteretic) model serves as a numerical example for demonstrating the efficiency of the proposed methodology. Note that the proposed framework can be applied in a straightforward manner to address cases of more sophisticated hysteretic modeling as well (e.g. enhanced Bouc-Wen, and Preisach models). However, the framework is limited to nonlinear/hysteretic modeling/functions for which equivalent linear elements can be determined via a statistical linearization approach.

REFERENCES

[1] Roberts J. B., Spanos P. D., Random vibration and statistical linearization, New York: Dover Publications, 2003.

[2] Soong T. T., Grigoriu M., Random vibrations of mechanical and structural systems, Prentice-Hall, New Jersey, 1993.

[3] Li J., Chen J., Stochastic dynamics of structures, New York: Dover Publications, 2009.

[4] Ellingwood B., Earthquake risk assessment of building structures, Reliab. Eng. Syst. Saf.;74: 251–62, 2001.

[5] Porter K. A., An overview of PEER's performance-based earthquake engineering methodology. Proceedings of the ninth international conference on applications of statistics and probability in civil engineering (ICASP9), 2003 July 6–9, San Francisco, USA. Rotterdam: Millpress; pp.973–80, 2003.

[6] Wen Y. K., Kang Y. J., Minimum building life-cycle cost design criteria. I: methodology, J Struct Eng; 127(3): 330-7, 2001.

[7] Kong J. S., Frangopol D. M., Life-cycle reliability-based maintenance cost optimization of deteriorating structures with emphasis on bridges, J Struct Eng; 129(6):818–28, 2003.

[8] Ang A. H-S., Lee J-C., Cost optimal design of R/C buildings. Reliab Eng System Safe; 73:233–8, 2001.

[9] Fragiadakis M., Lagaros N. D, Papadrakakis M., Performance-based multiobjective optimum design of steel structures considering life-cycle cost, Structural and Multidisciplinary Optimization; 32:1-11, 2006.

[10] Liu M., Burns S. A., Wen Y. K., Optimal seismic design of steel frame buildings based on life cycle cost considerations, Earthquake Eng Struct Dynamics; 32:1313–32, 2003.

[11] Taflanidis A. A., Beck J. L., Life-cycle cost optimal design of passive dissipative devices, Struct Safe; 31: 508-22, 2009.

[12] Takahashi Y., Der Kiureghian A., Ang A. H-S., Life-cycle cost analysis based on a renewal model of earthquake occurrences, Earth Eng Struct Dyn; 33(7): 859–80, 2004.

[13] Vamvatsikos D, Cornell CA., Incremental dynamic analysis, Earthquake Engineering and Structural Dynamics; 31:491–514, 2002.

[14] Au S. K., Beck J. L., Subset simulation and its application to seismic risk based on dynamic analysis, Journal of Engineering Mechanics (ASCE); 129:901–917, 2003.

[15] Rubinstein R. Y., Simulation and the Monte Carlo Method, Wiley, 1981.

[16] Schueller, G. I., Pradlwarter, H. J., and Koutsourelakis, P. S., A Critical Appraisal of Reliability Estimation Procedures for High Dimensions, Probab. Eng. Mech., 19, pp. 463–474, 2004.

[17] Lutes L. D., Sarkani S., Random Vibrations: Analysis of Structural and Mechanical Systems. Elsevier Butterworth-Heinemann: Burlington, MA, 2004.

[18] Kougioumtzoglou I. A., Spanos P. D., Nonlinear MDOF system stochastic response determination via a dimension reduction approach, Computers and Structures; 126: 135-148, 2013.

[19] Fujimura K., Der Kiureghian A., Tail-equivalent linearization method for nonlinear random vibration, Probab. Eng. Mech; 22:63–76, 2007.

[20] Der Kiureghian A., Fujimura K., Nonlinear stochastic dynamic analysis for performance-based earthquake engineering, Earthquake Engng Struct. Dyn.; 38:719–738, 2009.

[21] Jensen H. A., Tradeoff analysis of non-linear dynamical systems under stochastic excitation, Probab. Eng. Mech; 24: 585-599, 2009.

[22] Dahlhaus R., Fitting time series models to non-stationary processes, Ann Stat; 25: 1–37,1997.

[23] Hammond J.K., Evolutionary spectra in random vibration, J Roy Stat Soc; 35: 167–188. 1973.

[24] Jangid R. S., Datta T. K., Evaluation of the methods for response analysis under non-stationary excitation, Shock and Vibration; 6: 285–297, 1999.

[25] Spanos P. D., Solomos G. P., Markov approximation to transient vibration, J Eng Mech;109: 1134–50, 1983.

[26] Spanos P. D., Lutes L. D, Probability of response to evolutionary process, J. Eng Mech. Div. Am. Soc. Civil Eng., 106, 213-224, 1980.

[27] Spanos P. D., Non-stationary random vibration of a linear structure, International Journal of Solids and Structures, vol 14: 861-867, 1978.

[28] Caughey T. K., Random excitation of a system with bilinear hysteresis, Journal of Applied Mechanics, ASME, 27, 649-652, 1960.

[29] Giaralis, A., Spanos, P. D., Effective linear damping and stiffness coefficients of nonlinear systems for design spectrum based analysis. Soil Dynamics and Earthquake Engineering, 30: 9 798-810, 2010.

[30] Tubaldi E., Kougioumtzoglou I. A., Nonstationary stochastic response of structural systems equipped with nonlinear viscous dampers under seismic excitation, Earthquake Engng Struct. Dyn, DOI: 10.1002/eqe.2462, 2014.

[31] Solomos G. P., and Spanos P. D., Structural reliability under evolutionary seismic excitation, Soil Dynamics and Earthquake Engineering, 2: 110-16, 1983.

[32] Spanos P. D., Kougioumtzoglou I. A., Survival probability determination of nonlinear oscillators subject to evolutionary stochastic excitation, ASME J Appl. Mech., 81(5),051016 1–9, 2014.

[33] Ang A. H-S., Tang W.H., Probability concepts in engineering, 2nd edition Wiley, 2007.

[34] Au S. K., Beck J. L., First excursion probabilities for linear systems by very efficient importance sampling, Probabilistic Engineering Mechanics 16, pp. 193-207, 2001.

[35] Cornell C. A., Krawinkler H., Progress and challenges in seismic performance assessment, PEER Center News; Spring 2000. http://peer.berkeley.edu/news/ 2000spring/index.html.

[36] Mohle J., Deierlein G. G., A framework methodology for performance-based earthquake engineering, Proceedings13th World Conference on Earthquake Engineering, Paper No 679, Vancouver, B,C., Canada, 2004.

[37] Cornell C. A., Jalayer F., Hamburger R., Foutch D., Probabilistic basis for 2000 SAC federal emergency management agency steel moment frame guidelines, ASCE J Struct Eng; 128: 526–32, 2002.

[38] Ghobarah A., On drift limits associated with different damage levels. In: Fajfar P., Krawinkler H. (eds) International workshop on performance-based seismic design. Bled, Slovenia, 2004.

[39] Ellingwood B, Wen Y. K., Risk-benefit-based design decisions for low probability/high consequence earthquake events in Mid-America. Prog Struct. Eng. Mater (7):56–70, 2005.

[40] Deb K., Pratap A., Agarwal S., Meyarivan T., A fast and elitist multiobjective genetic algorithm: NSGA-II. IEEE Trans Evol. Comput. 6(2):182–197, 2002.

[41] Bäck T., Schwefel H.P., An overview of evolutionary algorithms for parameter optimization. Evol. Comput., 1(1), 1-23, 1993.

[42] Ikhouane F., Rodellar J., Systems with hysteresis: analysis, identification and control using the Bouc-Wen model, John Wiley and Sons, 2007.

[43] Clough R. W., Penzien J., Dynamics of structures, McGraw-Hill, 1993.

[44] Shinozuka M., Deodatis G., Simulation of stochastic processes by spectral representation, Applied Mechanics Reviews, vol. 44, no. 4, pp. 191-204, 1991.